2P5-16

Proceedings of Symposium on Ultrasonic Electronics, Vol. 30 (2009) pp. 351-352
18-20 November, 2009

Evaluation for Tissue Boundary Imaging Based on Motion Vector
動きベクトルに基づく組織境界イメージングの評価

Hironari Masui[1†], Takashi Azuma[1] and Kazuaki Sasaki[2]
([1]Hitachi CRL, [2]Tokyo Univ. of A&T)
増井裕也[1†]，東隆[1]，佐々木一昭[2]　([1]日立 中研, [2]農工大 農)

1. Introduction

Defining the boundary between a tumor and the normal tissue surrounding it is essential for non- and minimally invasive therapies. Tissue strain imaging is effective for tissue characterization [1] and it is possible to transform it to a color map, but this involves a computational complexity. Tissue boundaries on color maps are not always clearly defined, because nonlinearity exists in the transformation [2]. Various studies using a correlation-based method have recently been conducted to measure the elastic properties [3]. Several groups have studied the vector maps of tissue motion to investigate tissue elasticity [4].

We have proposed a ultrasonic straingraphy that is based on detecting the spatial discontinuity in the tissue motion vector [5,6], which is estimated by using the correlation of images between sequential frames [7]. We used eigenvalue decomposition technique to transform from a vector map to a scalar one [8].

We introduce four different analysis methods in this paper for detecting the spatial discontinuity in the motion vector: divergence, rotation, strain tesor, and eigenvalue decomposition analyses. These methods are evaluated by comparison in vivo and vitro.

2. Motion Vector Imaging

A motion vector is detected from two image frames based on block matching. A window array, which is the search area, is set in each frame to measure motion. We set the region of interest (ROI) at the size of a speckle caused by ultrasonic measurement. We selected a 30×30 pixel size as our region. We found that the best region for matching was from a 50×50 pixel search area that was set in the next frame by searching for the minimum points for a sum of absolute differences (SAD).

There can be error vectors in a mothion vector map in the block matching process, because there can be a low SNR in a B-mode movie. These error vectors cause pseudo boundaries in a scalar map. To avoid this disadvantage, unreliable vectors need to be omitted from the motion vector mapping. A reliability evaluation can be performed by using a SAD distribution feature parameter; e.g., the variation coefficient of the distribution.

After the motion vector is mapped, an image processing is used to detect any spatial discontinuity. Four imaging methods are tested: divergence, rotation, strain tensor, and eigenvalue decomposition analyses. Our divergence method is a weighted one that corresponds to the axial direction because a point spread function (PSF) blurs in the rateral direction. Rotation reflects shear strain at a discontinuous boundary. A strain tensor corresponds to a separation of two points in two frames. Eigenvalue decomposition method used maximum absolute value of eigenvalues. A ROI size of 3×3 pixels was selected for all imaging methods according to a muximum dimension of the feature space in the analysis.

3. Experimental Results

In our phantom experiments, the imaging methods were compared by using a two-layered phantom. **Figure 1(a)** shows a B-mode image. The lower layer is shifting laterally, while the upper layer is in a static condition relatively.

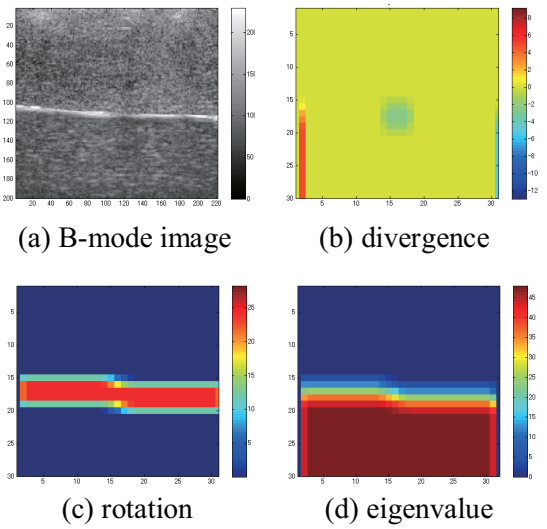

(a) B-mode image　(b) divergence

(c) rotation　(d) eigenvalue

Fig. 1　Two-layered phantom

It was difficult for the divergence method to respond to the laterally-shifted border, as shown in Fig. 1(b). The rotation method (Fig. 1(c)) clearly indicates the border. The strain tensor method shows the results just as well as the rotation one. The eigenvalue decomposition method (Fig. 1(d)) reflected the characterization of each region.

A VX2 tumor implanted in the liver of a rabbit and a biceps brachii muscle of a human volunteer were chosen as the test subjects in vivo. An EUB-8500 ultrasonic scanner (Hitachi Medical Corp., Tokyo, Japan), hand-held fixing linear array probe EUP-L54M, and EUP-L65 (Hitachi Medical Corp., Tokyo, Japan) were used to obtain the image frames. The probes were operated at a frequency of 9 MHz.

Figure 2 shows a B-mode image and a vector map of the tissue motion for the VX2 tumor implanted in rabbit liver. These are decimated to 1/2.

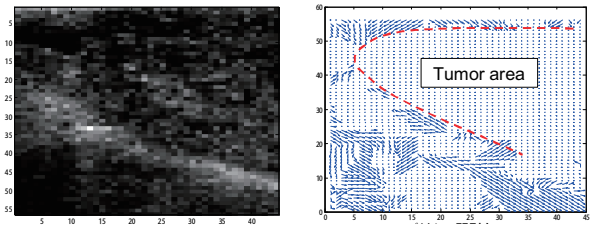

(a) B-mode image (b) vector map

Fig. 2 VX2 tumor implanted in rabbit liver

Figure 3 shows the scalar component computed from the vector map. Figure 3(a) is obtained by using the divergence method. This ensures there is boundary continuity between the tumor and surrounding normal tissue. The rotation method, which is shown in Fig. 3(b), lacked continuity, but was well accorded with the vector map.

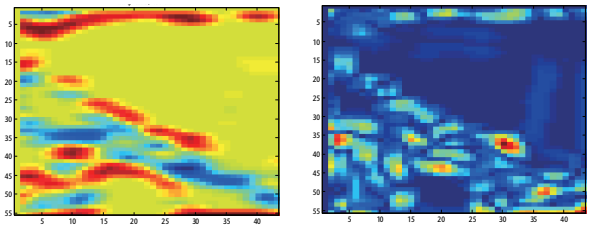

(a) divergence (b) rotation

Fig. 3 Boundary imaging

Figure 4 shows a B-mode image and a vector map of the tissue motion for the human biceps brachii muscle. These are decimated to 1/2 and 1/4, respectively. The muscle boundary was unclear in the B-mode image. According to the vector map, the image consists of two regions.

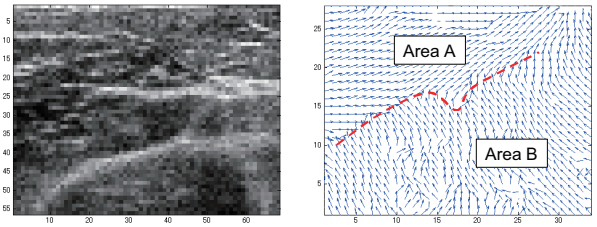

(a) B-mode image (b) vector map

Fig. 4 Biceps brachii muscle

Figure 5(a) was obtained by using the strain tensor method. The boundary was clearly detected, but there is partially noise in the image. The eigenvalue decomposition, which is in Fig. 5(b), shows there is a fine border and little noise. It sufficiently reflects vector map information.

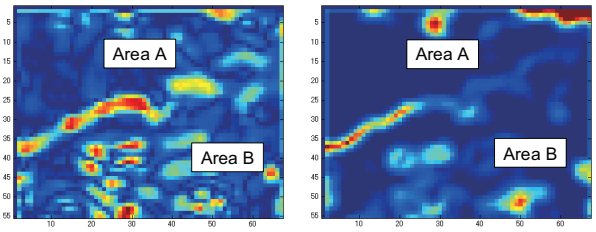

(a) strain tensor (b) eigenvalue

Fig. 5 Boundary imaging

4. Conclusion

We proposed boundary imaging methods that are based on the motion vector and conducted a phantom experiment to compare the characteristics of the four techniques. An VX2 tumor implanted in the liver of a rabbit and a human biceps brachii muscle were used in our verification experiments. It is important to optimize the imaging method according to diagnostic region.

References

1. T. Shiina et al.: J. Med. Ultrason. **29** (2002) 119.
2. N. Nitta et al.: IEICE **J84-A** (2001) 1405 (in Japanese).
3. H. Hasegawa and H. Kanai: Proc. IEEE Ultrason. Symp. (2008) 225.
4. Y. Yamashita and M. Kubota: Proc. IEEE Ultrason. Symp. (1990) 1371.
5. T. Azuma et al.: Proc. IEEE Ultrason. Symp. (2006) 2040.
6. H. Masui et al.: Proc. Symp. Ultrason. Electron. **28** (2007) 429.
7. H. Yoshikawa et al.: Jpn. J. Appl. Phys. **45** (2006) 4754.
8. H. Masui et al.: Proc. Symp. Ultrason. Electron. **29** (2008) 285.